Large deformation finite element modelling of single-curvature composite sheet forming with tool contact

S.P. McEntee & C.M. Ó Brádaigh

Composites Research Unit, Department of Mechanical Engineering, University College Galway, Ireland

Abstract

A finite element model for sheet forming of unidirectional continuous fibre reinforced composite laminates, which incorporates large deformation contact elements for modelling tool contact and interply slip, is presented. The composite plies are assumed to behave as an ideal fibre reinforced fluid, having the constraints of inextensibility in the fibre direction and material incompressibility. A finite element model has previously been developed which can simulate large deformations of an ideal fibre reinforced fluid body in plane strain using a quasi-static approach. This model is extended in this paper to include interply effects and tool contact by using special contact finite elements. The potential of the model is illustrated using test case simulations.

1 Introduction

Sheet forming manufacturing processes are a means by which composite laminates can be formed into a variety of complex curvilinear shapes [1]. Thermoset composite forming, widely known as the 'hot-draping' process, is seen a cost-effective alternative to hand-layup of prepreg over tool surfaces. Thermoplastic composite forming, in particular diaphragm forming and press forming, can provide an effective means of producing finished structural shapes in a single moulding process involving heating, forming, and cooling. However, forming such a highly constrained material as a continuous fiber composite laminate presents considerable difficulties. Fiber buckling, fiber washing, void formation and warping are some of the problems that must be avoided if a component is to be formed successfully. The quality of a press formed component will depend on many factors such as mould design, laminate lay-up, forming rate and temperature etc. Software tools that simulate the press forming process can assist the designer by allowing a prediction of the final part quality, and can help avoid the traditional (and expensive) trial and error design procedure.

A unidirectional continuous fiber composite consists, during the forming process, of very stiff, continuous, highly collimated fibers embedded in a relatively compliant matrix. The matrix may be a thermoplastic, in which case the forming takes place above the melt temperature of the polymer. It may also be an uncured thermoset matrix, in which case the forming is carried out at temperatures between 50°C and 100°C, where the matrix is soft but not quite molten.

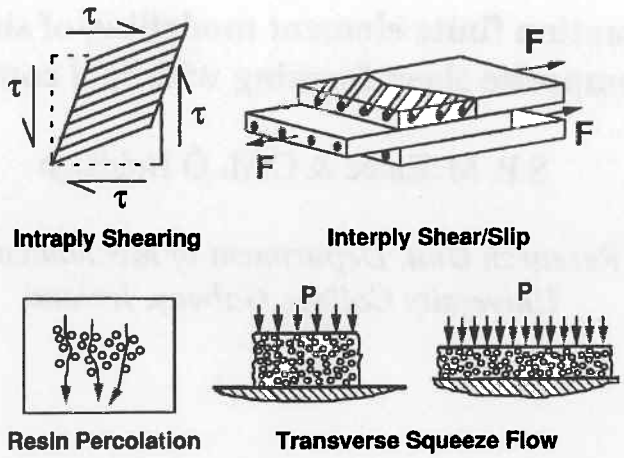

Fig. 1 Important forming mechanisms for unidirectional composites.

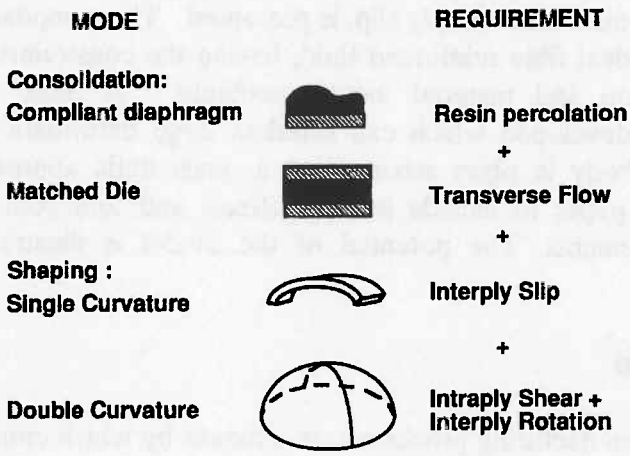

Fig. 2 Hierarchy of forming mechanisms needed for components of increasing complexity.

The dominant characteristic of both these types of materials is the very high viscosity in the fiber direction compared to other unreinforced directions. The fiber directions may be considered inextensible during flow, resulting in a material which deforms primarily in shear, along and transverse to the fiber direction. This situation is further complicated in reality as all practical laminates will have plies of more than one fiber orientation, all with different inextensible directions.

Figure 1 illustrates the forming mechanisms observed in these processes. The two main shearing mechanisms are the intraply mode, where fibers within each ply move past each other in the plane of the ply; and the interply mode, where plies that cannot stretch in a particular direction slide over each other in order to achieve a laminate curvature. Secondary mechanisms include transverse flow of fibers and matrix material in response to pressure gradients, and resin percolation, more often seen with thermoset matrix materials than with thermoplastics. Fabric reinforced composites have other forming mechanisms which will not be dealt with in this paper. Figure 2 shows the hierarchy of mechanisms that is needed to form particular shapes. For simple consolidation between matched metal dies, transverse flow and resin percolation are sufficient. For single-curvature forming, interply slip is needed to allow for fiber

inextensibility, whereas for double-curvature forming, all four mechanisms are needed to match the material to the complex surface. The formulation presented here is capable of modelling intraply and interply shear, but does not model resin percolation, or transverse flow in the mould axis direction. Also, the formulation does not allow for transverse flows of plies whose angles are other than 90°. However, it is felt that, as most thickness changes in the 1-3 plane are due to transverse flows in the 90° plies, rather than in the angle plies, the model is not unduly restricted.

The model presented here will deal with single-curvature forming situations only. These are an important class of sheet-formed products, including J-beams, U-beams, sine-wave spars, and Z-stiffeners for aerospace applications, some of which are illustrated in Figure 3. The key deformation mechanisms here are the slip between the plies and the transverse flow within each ply in response to pressure gradients as the material contacts the tool. In particular, the assumption of plane strain, or plane deformation conditions, in the plane transverse to the axis of the component is employed (i.e. the 1-3 plane). This assumption is appropriate for regions near the centre of a long prismatic shape, as shown denoted by section A-A in Figure 3, rather than at the ends (sections B-B and C-C), where flows along the component axis (in the 2 direction) may also occur.

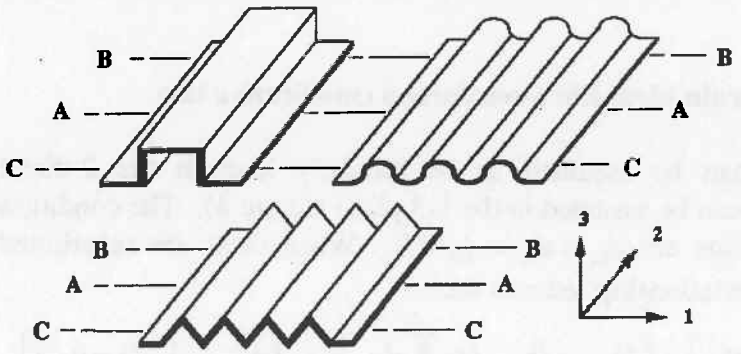

Fig. 3 Typical single-curvature components that are formed from flat composite sheets.

Finite element modelling of composite sheet forming processes has taken two routes - the implicit and explicit approaches. The explicit method has been applied by Pickett et al. [2] as part of an overall programme in the simulation of composite press-forming. The implicit method, which may be more suitable for slower forming situations, has been developed by Ó Brádaigh and co-workers for plane-stress [3,4] and plane strain [5,6] flow situations.

2 The ideal fibre reinforced fluid model

Rogers [7] introduced the ideal fibre reinforced fluid (IFRF) constitutive model for unidirectional continuous fibre reinforced composite melts. This model assumes that the material behaves as an anisotropic Newtonian fluid with the constraints of inextensibility in the fibre direction and material incompressibility. This constitutive model is used as the basis for the present formulation.

The IFRF constitutive relationship is, in indicial notation with repeated suffix summation, for $(i, j = 1,2,3)$ [7]:

$$\sigma_{ij} = -p(\delta_{ij} - a_i a_j) + Ta_i a_j + 2\eta_T d_{ij} + 2(\eta_L - \eta_T)(a_i a_k d_{kj} + a_j a_k d_{ik}) \qquad (1)$$

$\boldsymbol{a}$ is a unit vector representing the local fibre direction; $\boldsymbol{d}$ is the Eulerian rate-of-strain tensor; δ_{ij} is the Kronecker delta ($\delta_{ij} = 1$, i = j; $\delta_{ij} = 0$, i ≠ j); σ is the stress tensor; η_L is the longitudinal shear viscosity; η_T is the transverse shear viscosity; p is an arbitrary hydrostatic pressure; and T is an arbitrary tension in the fibre direction.

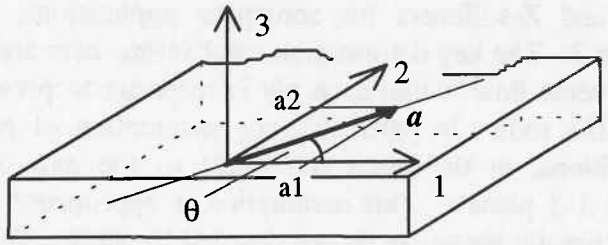

Fig. 4 The co-ordinate system axes and the unit fibre direction vector. θ is the ply fibre angle. Initially, the IFRF ply lies in the 1-2 plane, and thus $a_3 = 0$ when $t = 0$. Once deformation begins the a_3 becomes non-zero.

2.1 Plane strain ideal fibre-reinforced constitutive law

If the ply can be assumed to be infinitely long in the 2-direction, then plane deformation can be assumed in the 1-3 plane (figure 4). The conditions for plane strain in the 1-3 plane are $d_{22} = d_{23} = d_{12} = 0$. When these are substituted into eqn(1) the constitutive relationship reduces to:

$$\begin{bmatrix} \sigma_{11} \\ \sigma_{33} \\ \sigma_{13} \end{bmatrix} = \begin{bmatrix} D_{11} & 0 & D_{13} \\ 0 & D_{22} & D_{23} \\ D_{31} & D_{32} & D_{33} \end{bmatrix} \begin{bmatrix} d_{11} \\ d_{33} \\ 2d_{13} \end{bmatrix} + \begin{bmatrix} Ta_1^2 \\ Ta_3^2 \\ Ta_1 a_3 \end{bmatrix} - \begin{bmatrix} p(1-a_1^2) \\ p(1-a_3^2) \\ -pa_1 a_3 \end{bmatrix} \qquad (2)$$

where
$$D_{11} = 2\eta_T + 4(\eta_L - \eta_T)a_1^2$$
$$D_{22} = 2\eta_T + 4(\eta_L - \eta_T)a_3^2$$
$$D_{33} = \eta_T + (\eta_L - \eta_T)(a_1^2 + a_3^2)$$
$$D_{23} = D_{32} = D_{13} = D_{31} = 2(\eta_L - \eta_T)a_1 a_3$$

As this formulation is being developed to model fundamental shearing flows, dynamic terms are omitted from the equilibrium equations, and the problem is treated as being static over the flow domain Ω. When modelling actual forming flows the flow domain becomes a function of time, $\Omega(t)$. If the viscous forces dominate the forming flow, which is the case for many sheet forming situations, the dynamic terms can still be neglected, and the problem can be treated in a quasi-static fashion over the time domain t. The equilibrium and boundary traction equations become:

$$\sigma_{ij,j} = 0 \text{ in } \Omega$$
$$\bar{t}_j = n_i \sigma_{ij} \text{ on } \Gamma_t \quad (i, j = 1,3) \qquad (3)$$

where Γ_t is the boundary on which the tractions $\bar{t}$ are prescribed, n is the unit normal vector on the boundary. Body forces are neglected in the present formulation.

2.2 Plane strain IFRF finite element formulation

A finite element formulation for modelling flow in an ideal fibre reinforced Newtonian fluid in plane strain has been developed. Details of the derivation of this formulation are given elsewhere [5]. The formulation uses the mixed penalty method:

$$\begin{bmatrix} \mathbf{K}^v & \mathbf{K}^t & \mathbf{K}^p \\ (\mathbf{K}^t)^T & -\frac{1}{\alpha^t}\mathbf{M}^t & 0 \\ (\mathbf{K}^p)^T & 0 & -\frac{1}{\alpha^p}\mathbf{M}^p \end{bmatrix} \begin{Bmatrix} \phi^v \\ \phi^t \\ \phi^p \end{Bmatrix} = \begin{Bmatrix} \mathbf{f} \\ 0 \\ 0 \end{Bmatrix} \tag{4}$$

ϕ^v, ϕ^t, and ϕ^p are vectors of nodal velocities, fibre tensions, and pressures respectively. The velocity, fibre tension, and pressure field are discretized independently: $v \approx \hat{v} = \mathbf{N}^v\phi^v$; $T \approx \hat{T} = \mathbf{N}^t\phi^t$; $p \approx \hat{p} = \mathbf{N}^p\phi^p$; where $\mathbf{N}^v$, $\mathbf{N}^t$, and $\mathbf{N}^p$ are matrices of the interpolation functions for velocity, fibre tension, and pressure respectively. The matrices in eqn(4) are given by:

$$\mathbf{K}^v = \int_\Omega (\mathbf{B}^v)^T \mathbf{D}\mathbf{B}^v \, d\Omega \qquad \mathbf{K}^t = \int_\Omega (\mathbf{B}^v)^T \mathbf{a}\mathbf{N}^t \, d\Omega$$

$$\mathbf{K}^p = \int_\Omega (\mathbf{B}^v)^T [\mathbf{m} - \mathbf{a}]\mathbf{N}^p \, d\Omega \qquad \mathbf{f} = \int_\Gamma (\mathbf{N}^v)^T \bar{\mathbf{t}} \, d\Gamma$$

and $$\mathbf{M}^t = \int_\Omega (\mathbf{N}^t)^T \mathbf{N}^t \, d\Omega \qquad \mathbf{M}^p = \int_\Omega (\mathbf{N}^p)^T \mathbf{N}^p \, d\Omega$$

The $\mathbf{B}^v$ matrix is defined from the strain rate definition as: $\dot{\varepsilon} \approx \hat{\dot{\varepsilon}} = \mathbf{B}^v\phi^v$. The $\mathbf{D}$ matrix is the 3×3 matrix given in eqn(2). The column matrices $\mathbf{a}$ and $\mathbf{m}$ are:

$$\mathbf{a} = \langle a_1^2 \quad a_3^2 \quad a_1 a_3 \rangle^T \qquad \mathbf{m} = \langle 1 \quad 1 \quad 0 \rangle^T \tag{5}$$

α^t and α^p are scalar penalty numbers for fibre tension and pressure respectively. The constraints of fibre inextensibility and incompressibility are enforced exactly as $\alpha^t \to \infty$ and $\alpha^p \to \infty$. The formulation uses a Q 9/4/4 element. This element utilises a biquadratic velocity interpolation function, and discontinuous bilinear interpolation functions for the fibre tension and pressure. The fibre tension and pressure nodes are located inside the element at the 2×2 Gaussian integration points. All the element matrices are calculated using full 3×3 Gaussian integration. The values $\eta_L = 8000$ Pa.s, $\eta_T = 6000$ Pa.s, $\alpha^t = 10^{12}$, and $\alpha^p = 10^{11}$ were used in all the examples in this paper.

3 Kinematic constraint updating scheme

An ideal fibre reinforced fluid is a kinematically highly constrained material. This is even more true when the plane strain condition is added. Rogers [8] states that for an IFRF under plane strain conditions "*when the position of one particle on each fibre is*

given, the positions of the others along the fibre are obtained from the inextensibility condition." Given that the fibres are all parallel and remain so during deformation, this suggests that if a single point on an IFRF ply is defined then all the other material points can be found, for a given set of boundary conditions, based on the kinematic constraints alone. A large deformation finite element formulation has previously been developed [6] which exploits the constrained nature of an IFRF body in plane strain in order to maintain the IFRF kinematic constraints of incompessibility and fibre inextensibility during mesh updating of quasi-static solution steps of the formulation given by eqn(4). The approach adopted is as follows. By judiciously selecting one or a few points on an IFRF ply and integrating the velocity, (obtained from eqn(4),) to find the displacements at these points, the kinematically correct geometry for the entire ply can be followed during large deformation mesh updating.

3.1 Kinematics

A material point's co-ordinates can be defined in terms of the time and its reference condition: $x_i = x_i(X_R, t)$, X_R is the point's position at $t = 0$, $(i = 1,3; R = 1,3)$. Similarly the fibre direction at a material point at $t = 0$ is given by the unit vector $a(X_R, 0) = A(X_R)$. The fibre direction at time t can be found from the deformation gradient:

$$a_i = \frac{\partial x_i}{\partial X_R} A_R \tag{6}$$

Note that $a_2 = A_2$ is constant for plane strain deformation in the 1-3 plane. The condition for large deformation incompressibility is [8]:

$$\left| \frac{\partial x_i}{\partial X_R} \right| = 1 \tag{7}$$

That is the determinant of the Jacobian matrix must be 1. The condition for large deformation fibre inextensibility is [8]:

$$\frac{\partial x_i}{\partial X_R} \frac{\partial x_i}{\partial X_S} A_R A_S = 1 \tag{8}$$

3.2 Large deformation finite element formulation for mesh updating

The kinematic updating formulation applies the kinematic constraints during mesh updating by penalising them directly at the nodal points. The reason for taking this approach is to obtain a good fibre direction distribution throughout the mesh. If the inextensibility constraint was integrated over the elements then each element would effectively have a single fibre direction, and this could conceivably lead to the mesh "locking" if the difference in fibre direction between adjacent elements became large. No attempt is made to model the constitutive behaviour of the material during the updating phase, the aim is to simply enforce the kinematic constraints.

The constraint conditions can be written as $\mathbf{C}\phi = 0$ where ϕ is the displacement solution vector and $\mathbf{C}$ is the constraint matrix. Thus from eqn(7) the large deformation constraint matrix for incompressibility $\mathbf{C}_p$ is given by:

$$\left[\cdots \;\vdots\; \frac{\partial N_j}{\partial X_1}+\frac{1}{2}\frac{\partial u_3}{\partial X_3}\frac{\partial N_j}{\partial X_1}-\frac{1}{2}\frac{\partial u_3}{\partial X_1}\frac{\partial N_j}{\partial X_3} \;\vdots\; \frac{\partial N_j}{\partial X_3}+\frac{1}{2}\frac{\partial u_1}{\partial X_1}\frac{\partial N_j}{\partial X_3}-\frac{1}{2}\frac{\partial u_1}{\partial X_3}\frac{\partial N_j}{\partial X_1} \;\vdots\; \cdots\right]\begin{bmatrix}\vdots\\ \phi_{1j}\\ \phi_{3j}\\ \vdots\end{bmatrix}=\mathbf{C}_p\phi=0 \quad (9)$$

where u_1, u_3 are the displacement components, and the N are the isoparametric shape functions. Similarly, the large deformation fibre inextensibility constraint matrix $\mathbf{C}_t$ can be found from eqn(8):

$$\begin{bmatrix}\cdots & \vdots & A_1^2\left(2\frac{\partial N_j}{\partial X_1}+\frac{\partial u_1}{\partial X_1}\frac{\partial N_j}{\partial X_1}\right)+ & \vdots & A_3^2\left(2\frac{\partial N_j}{\partial X_3}+\frac{\partial u_3}{\partial X_3}\frac{\partial N_j}{\partial X_3}\right)+ & \vdots & \cdots\\ & & A_1A_3\left(2\frac{\partial N_j}{\partial X_3}+\frac{\partial u_1}{\partial X_1}\frac{\partial N_j}{\partial X_3}+\frac{\partial u_1}{\partial X_3}\frac{\partial N_j}{\partial X_1}\right)+ & & A_1A_3\left(2\frac{\partial N_j}{\partial X_1}+\frac{\partial u_3}{\partial X_3}\frac{\partial N_j}{\partial X_1}+\frac{\partial u_3}{\partial X_1}\frac{\partial N_j}{\partial X_3}\right)+ & & \\ & & A_3^2\frac{\partial u_1}{\partial X_3}\frac{\partial N_j}{\partial X_3} & & A_1^2\frac{\partial u_3}{\partial X_1}\frac{\partial N_j}{\partial X_1} & & \end{bmatrix}\begin{bmatrix}\vdots\\ \phi_{1j}\\ \phi_{3j}\\ \vdots\end{bmatrix} \quad (10)$$

$$=\mathbf{C}_t\phi=0$$

The constraint matrix can be written as $\mathbf{C}=\mathbf{FG}+\mathbf{EG}$. $\mathbf{F}$ defines the linear terms of the constraint matrix, $\mathbf{E}$ defines the non-linear terms. $\mathbf{G}$ consists of the global derivatives:

$$\mathbf{G}\phi=\begin{bmatrix}\frac{\partial N_j}{\partial X_1} & 0\\ 0 & \frac{\partial N_j}{\partial X_1}\\ \cdots & \cdots\\ \frac{\partial N_j}{\partial X_3} & 0\\ 0 & \frac{\partial N_j}{\partial X_3}\end{bmatrix}\begin{bmatrix}\vdots\\ \phi_{1j}\\ \phi_{3j}\\ \vdots\end{bmatrix}=\begin{bmatrix}\frac{\partial u_1}{\partial X_1}\\ \frac{\partial u_3}{\partial X_1}\\ \frac{\partial u_1}{\partial X_3}\\ \frac{\partial u_3}{\partial X_3}\end{bmatrix} \quad (11)$$

Thus the incompressibility constraint matrix is $\mathbf{C}_p=\mathbf{F}_p\mathbf{G}+\mathbf{E}_p\mathbf{G}$, where:

$$\mathbf{F}_p=\begin{bmatrix}1 & 0 & 0 & 1\end{bmatrix}$$
$$\mathbf{E}_p=\frac{1}{2}\begin{bmatrix}\frac{\partial u_3}{\partial X_3} & -\frac{\partial u_1}{\partial X_3} & -\frac{\partial u_3}{\partial X_1} & \frac{\partial u_1}{\partial X_1}\end{bmatrix} \quad (12)$$

Similarly, the constraint condition for fibre inextensibility can be written as $\mathbf{C}_t=\mathbf{F}_t\mathbf{G}+\mathbf{E}_t\mathbf{G}$, where from eqn(10) it can be seen that:

$$\mathbf{F}_t=2\begin{bmatrix}A_1^2 & A_1A_3 & A_1A_3 & A_3^2\end{bmatrix}$$
$$\mathbf{E}_t=\begin{bmatrix}A_1^2\frac{\partial u_1}{\partial X_1}+A_1A_3\frac{\partial u_1}{\partial X_3} & A_1^2\frac{\partial u_3}{\partial X_1}+A_1A_3\frac{\partial u_3}{\partial X_3} & A_3^2\frac{\partial u_1}{\partial X_3}+A_1A_3\frac{\partial u_1}{\partial X_1} & A_3^2\frac{\partial u_3}{\partial X_3}+A_1A_3\frac{\partial u_3}{\partial X_1}\end{bmatrix} \quad (13)$$

We follow the general approach outlined by Zienkiewicz & Taylor [9] for dealing with geometrically non-linear problems. We take a differential of the constraint equation: $\mathrm{d}(\mathbf{C}\phi)=\overline{\mathbf{C}}\,\mathrm{d}\phi$. For the incompressibility and fibre inextensibility constraints this leads to the respective definitions:

$$\overline{\mathbf{C}}_p=\mathbf{F}_p\mathbf{G}+2\mathbf{E}_p\mathbf{G} \qquad \overline{\mathbf{C}}_t=\mathbf{F}_t\mathbf{G}+2\mathbf{E}_t\mathbf{G} \quad (14)$$

The constraints are enforced by penalising them using penalty numbers α:

$$\lambda_p=\alpha_p\mathbf{C}_p\phi \qquad \lambda_t=\alpha_t\mathbf{C}_t\phi \quad (15)$$

These terms can be considered as Lagrange multipliers for the pressure and fibre tension. In order to employ the Newton Raphson technique a residual must first be found: $\Psi = \overline{\mathbf{C}}^{\mathrm{T}}\lambda$. To define the constraint components of the characteristic matrix the residual is linearised:

$$d\Psi = \overline{\mathbf{C}}^{\mathrm{T}}\, d\lambda + d\overline{\mathbf{C}}^{\mathrm{T}}\lambda = \alpha\overline{\mathbf{C}}^{\mathrm{T}}\overline{\mathbf{C}}\, d\phi + \mathbf{G}^{\mathrm{T}}\mathbf{M}\mathbf{G}\, d\phi = \overline{\mathbf{K}}\, d\phi + \mathbf{K}_{\sigma} d\phi \qquad (16)$$

$\mathbf{K}_{\sigma}$ is known as the *initial stress matrix* [9]. The $\mathbf{M}$ matrices can be found for the incompressibility and fibre inextensibility constraints by noting that $d\overline{\mathbf{C}}^{\mathrm{T}} = \mathbf{G}^{\mathrm{T}} 2\, d\mathbf{E}^{\mathrm{T}}$:

$$\mathbf{M}_p = \lambda_p \begin{bmatrix} 0 & 0 & 0 & 1 \\ 0 & 0 & -1 & 0 \\ 0 & -1 & 0 & 0 \\ 1 & 0 & 0 & 0 \end{bmatrix} \qquad \mathbf{M}_t = 2\lambda_t \begin{bmatrix} A_1^2 & 0 & A_1A_2 & 0 \\ 0 & A_1^2 & 0 & A_1A_2 \\ A_1A_2 & 0 & A_3^2 & 0 \\ 0 & A_1A_2 & 0 & A_3^2 \end{bmatrix} \qquad (17)$$

In theory, penalising the compressibility and the fibre extensibility should be sufficient to maintain the IFRF constraints, but in practice it is found that introducing the additional constraint of inextensibility in the direction normal to the fibre direction can significantly improve the results, particularly when the deformation becomes large. The condition of inextensibility in the direction normal to the fibre direction is the consequence of the incompressibility constraint in plane strain [8]. Inextensibility in the direction normal to the fibre direction is penalised in the same way as inextensibility in the fibre direction, except that a normal direction vector is used. This constraint is given the subscript n. The full updating formulation now becomes:

$$\left[\mathbf{K} + \overline{\mathbf{K}}_p + \mathbf{K}_{\sigma p} + \overline{\mathbf{K}}_t + \mathbf{K}_{\sigma t} + \overline{\mathbf{K}}_n + \mathbf{K}_{\sigma n}\right]\phi = \mathbf{R} - \mathbf{R}_p - \mathbf{R}_t - \mathbf{R}_n \qquad (18)$$

where

$$\overline{\mathbf{K}}_p = \alpha_p \overline{\mathbf{C}}_p^{\mathrm{T}}\overline{\mathbf{C}}_p \qquad \mathbf{K}_{\sigma p} = \mathbf{G}^{\mathrm{T}}\mathbf{M}_p\mathbf{G} \qquad \mathbf{R}_p = \overline{\mathbf{C}}_p^{\mathrm{T}}\lambda_p$$

$$\overline{\mathbf{K}}_t = \alpha_t \overline{\mathbf{C}}_t^{\mathrm{T}}\overline{\mathbf{C}}_t \qquad \mathbf{K}_{\sigma t} = \mathbf{G}^{\mathrm{T}}\mathbf{M}_t\mathbf{G} \qquad \mathbf{R}_t = \overline{\mathbf{C}}_t^{\mathrm{T}}\lambda_t$$

$$\overline{\mathbf{K}}_n = \alpha_n \overline{\mathbf{C}}_n^{\mathrm{T}}\overline{\mathbf{C}}_n \qquad \mathbf{K}_{\sigma n} = \mathbf{G}^{\mathrm{T}}\mathbf{M}_n\mathbf{G} \qquad \mathbf{R}_n = \overline{\mathbf{C}}_n^{\mathrm{T}}\lambda_n$$

The $\mathbf{K}$ matrix must be added so as to make the equation system non-singular. $\mathbf{R}$ contains the applied forces and residual terms due to $\mathbf{K}$. The $\mathbf{K}^{v}$ matrix given in eqn(4) has been used with $\eta_L = \eta_T = 1$ and $\alpha_p = \alpha_t = \alpha_n = 10^8$, in order to eliminate the anisotropy and minimise the effect of the $\mathbf{K}$ component on the solution. It can be calculated at the reduced integration points to save computational effort.

3.3 Overall solution scheme for kinematic mesh updating

The approach we take is to solve for the velocity field for each time step using the IFRF static formulation given by eqn(4). The boundary conditions where the velocity was constrained to zero are retained as zero displacement constraints. The force boundary conditions are discarded during the mesh updating phase. Next, one or a few degrees of freedom are selected as defining the mode of deformation, and these are used for the displacement constraints for a given time increment. These displacement constraints are used in the formulation given by eqn(18) to find the updated mesh for the next time step. Thus the mesh for the IFRF static formulation given by eqn(4) is updated in a quasi-static manner using the large deformation kinematic formulation

given by eqn(18). Results for test cases using this approach are given in an earlier paper [6].

4 Modelling interply slip and tool contact

When a multi-ply laminate is consolidated a "resin-rich" layer consisting of the matrix material forms between the plies. This layer is thin, for instance typically 10 μm thick between thermoplastic plies of 0.125 mm. Shear deformation in the interply layer is an important flow mechanism during the forming of curved components. Because the interply region is very thin compared to the thickness of a ply, it would be difficult to model this region using conventional continuum finite elements. Instead, the interply region is modelled using special contact finite elements. Thus, in order to model forming flows in multi-ply laminates, a mesh is created for each individual ply and these meshes are joined along the inter-ply region using contact elements. This approach has been used to model static forming flows in multiply laminates, treating the interply slip mechanism as a contact-friction phenomenon [5]. The fact that the kinematic updating formulation presented in section 3 is displacement based permits the use of large deformation contact finite elements to impose interply slip kinematic conditions during mesh updating. These kinematic conditions are simple: individual plies must not penetrate each other, nor should they separate (no attempt is made to model delamination.) Also, as with the kinematic updating formulation presented in section 3, no attempt is made to use a consititutive law to model interply slip during mesh updating. There is no contact friction during mesh updating, the only requirement is that the contact kinematic conditions are satisfied. The details of formulating contact finite elements are involved, and can be found elsewhere [10]. Details specific to the present formulation will be documented in future work.

Tool contact is also modelled using contact finite elements, except that the tool is allowed to separate from the work piece. Thus tool contact occurs only when the tool exerts a positive pressure on the work piece. This means that the only kinematic condition that needs to be satisfied during mesh updating is that tool nodes should not penetrate the work piece. Tools are assumed to be rigid, and to move in the 3-direction (vertical) only. Thus each tool can be treated as a single degree of freedom in the finite element formulation, the tool geometry being dealt with as a multi-point constraint. An advantage of using a tool is that it is not necessary to select degrees of freedom to be used as displacement boundary conditions during the kinematic updating stage. The tools themselves are the displacement boundary conditions during mesh updating.

5 Test cases

Figure 5 shows a model for a 3 point bend test. The punch and supporting roller are the "tools". A displacement of 100 mm/min is applied to the punch, while the roller is stationary. An analytical solution for this problem is given by Martin et al. [11], and this is compared to the finite element results in figure 6. A press forming simulation of a two ply laminate is shown in figure 7. There is a 7% error in the inextensibility constraint in this problem, a consequence of using a very large time step. It should be

possible to reduce this error to a more acceptable size by using smaller time steps in future work.

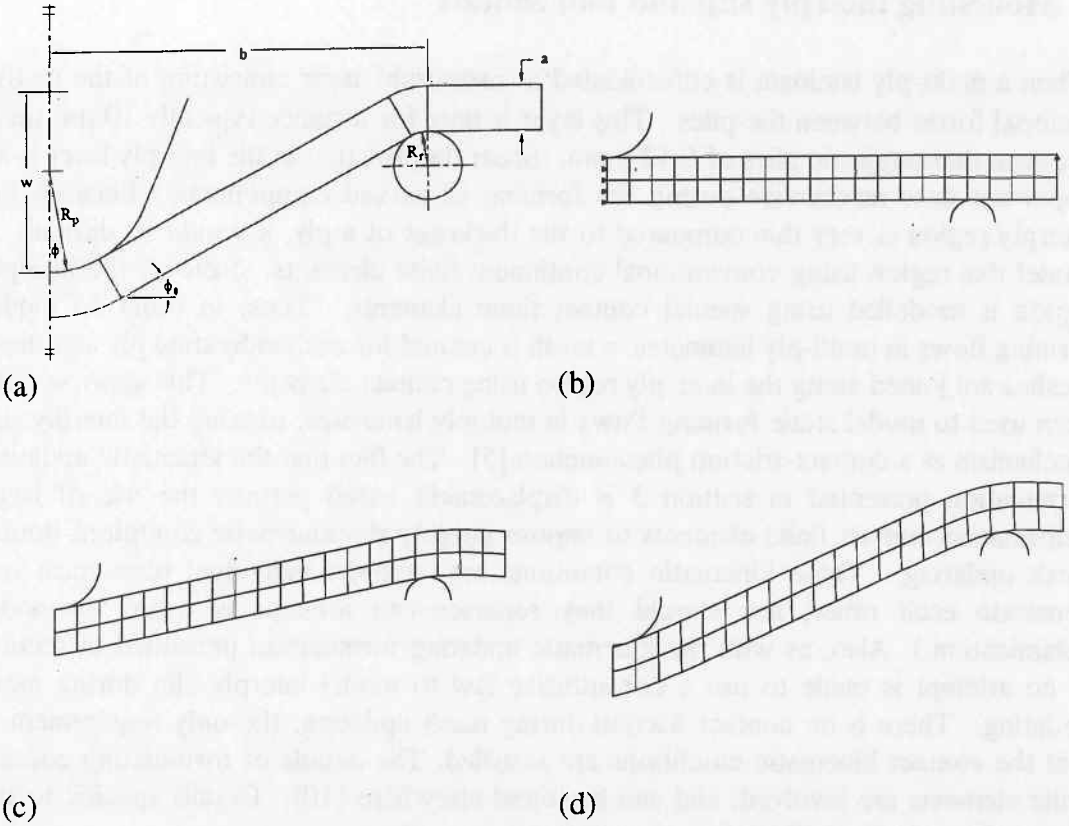

Fig. 5 (a) Model for 3 point bend test, adapted from Martin et al. [11]. (b) Finite element model for 3 point bend test of 0° IFRF beam. Length = 40 mm, a = 4 mm, b = 32.5 mm, R_r = 2 mm, R_p = 4 mm. Then punch (left) velocity is 100 mm/min. The roller (right) is stationary. Deformation shown after 4 s (c) and 8 s (d). The average errors for the IFRF kinematic constrains of inextensibility and incompressibility are less than 2%.

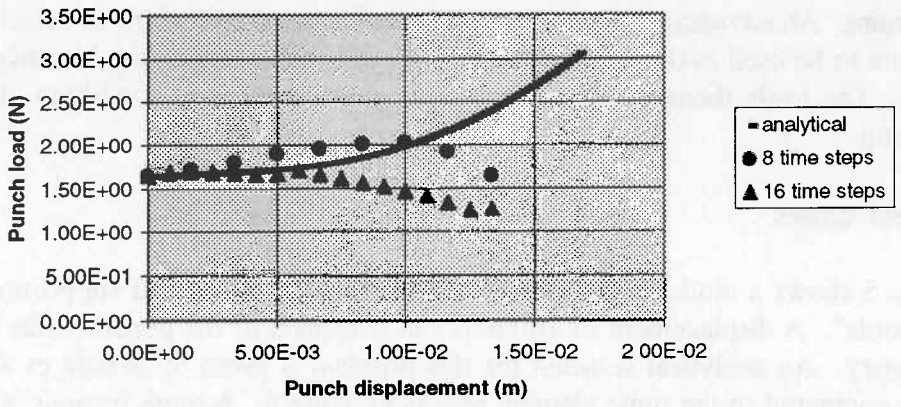

Fig. 6 Comparison between finite element results and analytical solution for 3 point bend test.

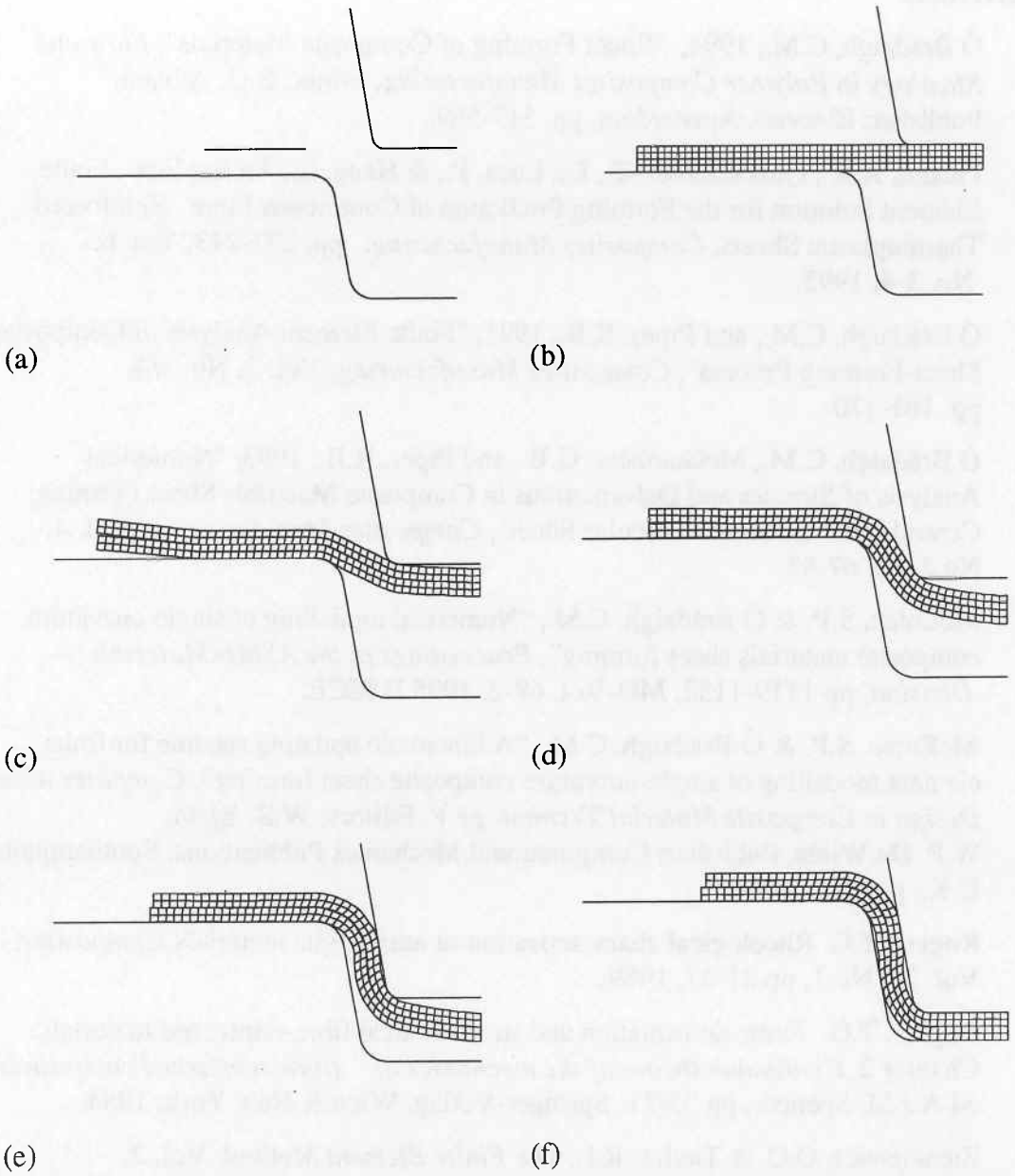

Fig. 7 Press forming test case. The work piece is a two ply laminate, both 0° plies. (a) The tool, consisting of stationary bottom piece, blank holder, and forming tool. The forming tool moves down at a constant velocity of 2.5 mm/s. (b) Time: 0 s. (c) Time: 1 s. (d) Time: 2 s. (e) Time: 3 s. (f) Time: 4 s. At the end of forming the average error over the two meshes for the IFRF kinematic constrains are: inextensibility 7%, incompressibility 2%.

6 Conclusion

A previously developed finite element formulation which can model large deformation sheet-forming of single curvature composite shapes was extended to included the interply slip mechanism in laminates, and tool contact, by the use of large deformation contact finite elements.

References

1. Ó Brádaigh, C.M., 1994, "Sheet Forming of Composite Materials", *Flow and Rheology in Polymer Composites Manufacturing*, Editor: S.G. Advani, Publisher: Elsevier, Amsterdam, pp. 517-569.

2. Pickett, A.K., Queckbörner, T., De Luca, P., & Hang, E., An Explicit Finite Element Solution for the Forming Prediction of Continuous Fibre Reinforced Thermoplastic Sheets, *Composites Manufacturing*, pp. 237-243, Vol. 6, No. 3-4, 1995.

3. Ó Brádaigh, C.M., and Pipes, R.B., 1991, "Finite Element Analysis of Composite Sheet-Forming Process", *Composites Manufacturing*, Vol. 2, No. 3/4, pp. 161-170.

4. Ó Brádaigh, C.M., McGuinness, G.B., and Pipes, R.B., 1993, "Numerical Analysis of Stresses and Deformations in Composite Materials Sheet Forming: Central Indentation of a Circular Sheet", *Composites Manufacturing*, Vol. 4, No.2, pp. 67-83.

5. McEntee, S.P. & Ó Brádaigh, C.M., "Numerical modelling of single-curvature composite materials sheet-forming", *Proceedings of the ASME Materials Division*, pp 1119-1132, MD-Vol. 69-2, 1995 IMECE.

6. McEntee, S.P. & Ó Brádaigh, C.M. "A kinematic updating scheme for finite element modelling of single-curvature composite sheet forming", *Computer Aided Design in Composite Material Technology V*, Editors: W.R. Blain, W.P. De Wilde, Publisher: Computational Mechanics Publications, Southampton, U.K., pp. 283-295.

7. Rogers, T.G. Rheological characterisation of anisotropic materials,*Composites*, Vol. 20, No.1, pp 21-27, 1989.

8. Rogers, T.G. Finite deformation and stress in ideal fibre-reinforced materials, Chapter 2, *Continuum theory of the mechanics of fibre-reinforced composites*, ed A.J.M. Spencer, pp 33-71, Springer-Verlag, Wien & New York, 1984.

9. Zienkiewicz, O.C. & Taylor, R.L. *The Finite Element Method*, Vol. 2, McGraw-Hill, London, 1991.

10. Laursen, T.A., and Simo, J.C., 1993, "A Continuum-Based Finite Element Formulation for the Implicit Solution of Multibody, Large Deformation Frictional Contact Problems", *International Journal for Numerical Methods in Engineering*, Vol. 36, pp. 3451-3485.

11. Martin, T.A., Bhattacharyya, D., and Collins, I.F., 1995, Bending of fibre-reinforced thermoplastic sheets", *Composites Manufacturing*, Vol. 6, No. 3-4, pp. 177-187.